THE EFFECT OF MUTUAL INDUCTANCE AND MUTUAL CAPACITANCE ON THE TRANSIENT RESPONSE OF BRAIDED-SHIELD COAXIAL CABLES*

David E. Merewether

T. F. Ezell

ABSTRACT

In this paper a quantitative comparison is made of the importance of mutual inductance and mutual capacitance in the leakage of transient signals through the braid of a coaxial cable. The difference between mutual inductance and mutual capacitance coupling is vividly exhibited in the transient predictions. Comparisons of predictions to measurements made on a length of RG-214 test cable are also included.

*This paper is based upon work supported by the ERDA under Sandia Laboratories Contract 33-1141.

INTRODUCTION

The generic form of the coupling through a braided-shield cable contains both mutual impedance (mutual resistance and inductance) and mutual admittance (capacitance) terms. Yet for most shielding measurements, either the "transfer impedance" or the "shielding effectiveness" is measured. In the first case, only the mutual impedance is measured and in the second case, a sum (or difference) of the mutual impedance and mutual admittance coupling is measured [1].

In many cases one is really only interested in the effectiveness of the shield. The dominant coupling mechanism is not of practical importance provided the transfer function between the undesired excitation and the response is accurate. The analyst may ask, "What difference does it make whether the mutual coupling is capacitive or inductive?" In this paper, we seek to answer that question: AC transfer functions are shown where it makes no difference what model is assumed and transient data is shown where the predicted response is markedly dependent upon the coupling model assumed.

Finally, the problem of measuring shield leakage and extrapolating to other cable configurations is discussed. Here mutual capacitance and mutual inductance are extrapolated in different ways.

Preceding these discussions, the formulation of the coupling problem for coaxial cables is reviewed and its solution reiterated.

FORMULATION

Whenever a coaxial cable is used in a system application, two circuits actually exist: The intended one formed by the inner conductor and the inside of the sheath and the spurious one formed by the outside of the sheath and its surroundings. For many configurations the outside circuit has many of the characteristics for a transmission line and the use of transmission line theory for both the inside and the outside circuit is appropriate. The coupled telegrapher's equations are [2]

$$\frac{\partial V_1}{\partial z} = -L_1 \frac{\partial I_1}{\partial t} + L_{ab} \frac{\partial I_2}{\partial t} - R_1 I_1 + R_{ab} I_2 + V_{s1} \tag{1}$$

$$\frac{\partial V_2}{\partial z} = -L_2 \frac{\partial I_2}{\partial t} + L_{ab} \frac{\partial I_1}{\partial t} - R_2 I_2 + R_{ab} I_1 + V_{s2} \tag{2}$$

$$\frac{\partial I_1}{\partial z} = -C_1 \frac{\partial V_1}{\partial t} - C_{ab} \frac{\partial V_2}{\partial t} - I_{s1} \tag{3}$$

$$\frac{\partial I_2}{\partial z} = -C_2 \frac{\partial V_2}{\partial t} - C_{ab} \frac{\partial V_1}{\partial t} - I_{s2} \tag{4}$$

Figure 1 shows how the voltages V_1, V_2 and currents I_1 and I_2 are to be defined in a typical triaxial measurement situation so that R_{ab}, L_{ab}, and C_{ab}, the parameters that control the coupling between the two lines are positive quantities. V_{s1}, V_{s2}, I_{s1}, I_{s2} are externally originated excitation sources that might include a signal generator, an incident electromagnetic field or ionizing radiation.

Simultaneous solution of the four equations is possible, however, for shielding problems the lines are loosely coupled ($C_{ab} \ll C_1$ or C_2, $L_{ab} \ll L_1$ or L_2) and considerable simplification results. Let us define line 1 to be the line excited by a source (either inside or outside) with time dependence $e^{+j\omega t}$. The problem is to determine the resultant voltages across the load Z_{L21} and Z_{L22}. For this case (1)-(4) reduce to:

$$\frac{\partial V_1}{\partial z} + (R_1 + j\omega L_1)\, I_1 = V_{s1}(z) \tag{5}$$

$$\frac{\partial I_1}{\partial z} + (j\omega C_1)\, V_1 = I_{s1}(z) \tag{6}$$

and

$$\frac{\partial V_2}{\partial z} + (R_2 + j\omega L_2)\, I_2 = (R_{ab} + j\omega L_{ab})\, I_1(z) \tag{7}$$

$$\frac{\partial I_2}{\partial z} + (j\omega C_2)\, V_2 = -j\omega C_{ab}\, V_1(z) \tag{8}$$

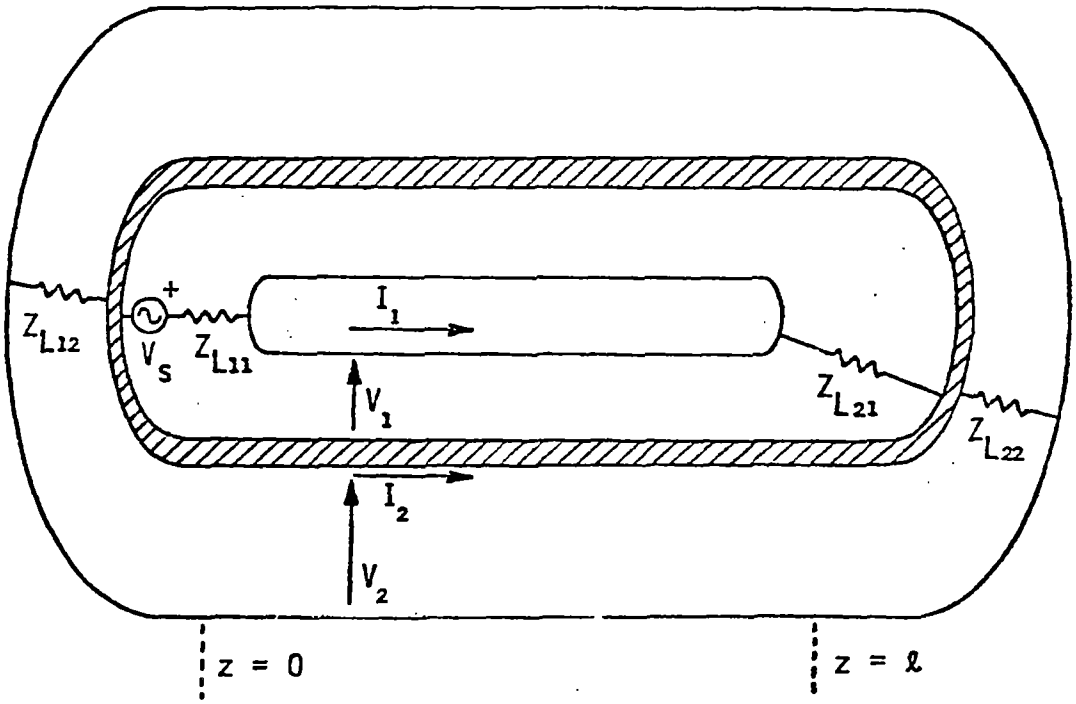

a. Physical configuration for measuring shield leakage for triaxial cable with elliptical end caps.

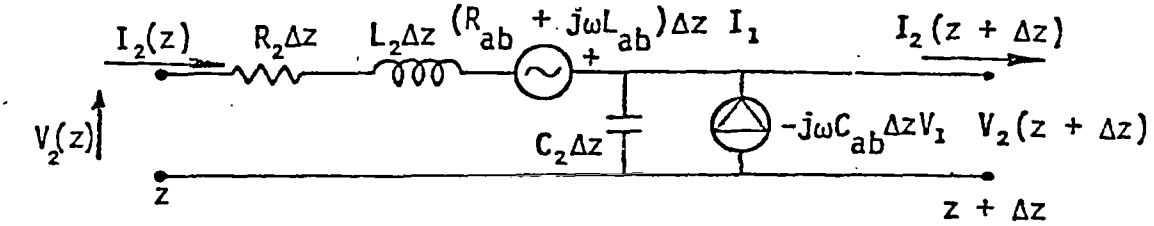

b. Equivalent circuit for an incremental length of outside circuit.

Figure 1

Here R_1 and R_2 are the AC resistance of the transmission lines in ohms/meter [3]. Note that the solution for V_1 and I_1 in (5) and (6) form the drive terms for (7) and (8). In solving either pair the solution for the response of a transmission line driven by distributed voltage and current sources is needed.

A simple way to solve inhomogeneous differential equations is the use of the "Green's function technique". In this approach the response of a linear system to a distributed source is computed by superposition of the responses obtained with a discreet source. Let $V^I(z,z')$ be the voltage V measured at z when the line is driven by a lumped shunt current source of one ampere at $z = z'$ and similarly let $V^V(z,z')$ be the voltage V measured at z when the line is driven by a lumped voltage source at $z = z'$.

The total response due to both current and voltage sources is

$$V(z) = \int_0^{\ell} V^I(z,z')\, I_s(z')dz' + \int_0^{\ell} V^V(z,z')\, V_s(z')dz' \qquad (9)$$

Similar formulas can be obtained for the current on the line

$$I(z) = \int_0^{\ell} I^I(z,z')\, I_s(z')dz' + \int_0^{\ell} I^V(z,z')\, V_s(z')dz' \qquad (10)$$

However, solution of either (9) or (10) is sufficient to determine the total response since if you know V(z) the current can be obtained from (5) or (7).

How to solve for the four "Green's Functions" is described adequately by Weeks [4]; only the results are given here. All four formulas are provided here because both the current and the voltage on line 1 are needed.

$$V^I(z,z') = \frac{Z_o}{2\Delta} e^{+\gamma(z-z')} [1 + \rho_1 e^{-2\gamma z}] [1 + \rho_2 e^{-2\gamma(\ell-z')}] \quad 0 \le z \le z'$$

$$= \frac{Z_o}{2\Delta} e^{-\gamma(z-z')} [1 + \rho_1 e^{-2\gamma z'}] [1 + \rho_2 e^{-2\gamma(\ell-z)}] \quad z' \le z \le \ell$$

(11)

and

$$V^V(z,z') = \frac{-1}{2\Delta} e^{+\gamma(z-z')} [1 + \rho_1 e^{-2\gamma z}] [1 - \rho_2 e^{-2\gamma(\ell-z')}] \quad 0 \le z \le z'$$

$$= \frac{1}{2\Delta} e^{-\gamma(z-z')} [1 - \rho_1 e^{-2\gamma z'}] [1 + \rho_2 e^{-2\gamma(\ell-z)}] \quad z' \le z \le \ell$$

(12)

$$I^I(z,z') = \frac{-1}{2\Delta} e^{+\gamma(z-z')} [1 - \rho_1 e^{-2\gamma z}] [1 + \rho_2 e^{-2\gamma(\ell-z')}] \quad 0 \le z \le z'$$

$$= \frac{1}{2\Delta} e^{-\gamma(z-z')} [1 + \rho_1 e^{-2\gamma z'}] [1 - \rho_2 e^{-2\gamma(\ell-z)}] \quad z' \le z \le \ell$$

(13)

$$I^V(z,z') = \frac{1}{2Z_o\Delta} e^{+\gamma(z-z')} [1 - \rho_1 e^{-2\gamma z}] [1 - \rho_2 e^{-2\gamma(\ell-z')}] \quad 0 \le z \le z'$$

$$= \frac{1}{2Z_o\Delta} e^{-\gamma(z-z')} [1 - \rho_1 e^{-2\gamma z'}] [1 - \rho_2 e^{-2\gamma(\ell-z)}] \quad z' \le z \le \ell$$

(14)

here

$$Z_o = \sqrt{\frac{(R + j\omega L)}{j\omega C}}, \quad \gamma = \sqrt{(R + j\omega L)(j\omega C)}$$

$$\rho_1 = \frac{Z_{L1} - Z_o}{Z_{L1} + Z_o}, \quad \rho_2 = \frac{Z_{L2} - Z_o}{Z_{L2} + Z_o} \qquad \text{(Reflection Coefficients)}$$

$$\Delta = (1 - \rho_1\rho_2 e^{-2\gamma\ell})$$

Subscripts will be added to these quantities to denote which line (1 or 2) is under consideration.

To obtain the line voltage for line 2, the Green's function would have to be applied twice to obtain $V_2(z)$ from Eq. (9).

$$V_2(z) = \int_0^{\ell} V_2^I(z,z')\ (-j\omega C_{ab} \cdot V_1(z'))dz \ + \int_0^{\ell} V_2^V(z,z')(R_{ab} + j\omega L_{ab}) \cdot I_1(z')dz' \tag{15}$$

$$= -j\omega C_{ab} \int_0^{\ell} V_2^I(z,z') \int_0^{\ell} [V_1^I(z',z'')\ I_{s1}(z'') + V_1^V(z',z'')\ V_{s1}(z'')]dz''\ dz'$$

$$+ (R_{ab} + j\omega L_{ab}) \int_0^{\ell} V_2^V(z,z') \int_0^{\ell} [I_1^I(z',z'')\ I_{s1}(z'')$$

$$+ I_1^V(z',z'')\ V_{s1}(z'')]dz''\ dz' \tag{16}$$

(16) is the general form of the response of the receiving line. Further manipulation of this equation is possible; however, little simplification is obtained until the distribution of the driving source is put into the equations. In the following we shall confine our interests to the case where a signal generator excites the driven line ($V_{s1} = V_s\delta(z)$, $I_{s1} = 0$), for which (from Eqs. (12) and (13))

$$V_1(z) = V_F\, e^{-\gamma_1 z} + V_R\, e^{+\gamma_1 z} \tag{17}$$

$$I_1(z) = Y_{o1}[V_F\, e^{-\gamma_1 z} - V_R\, e^{+\gamma_1 z}] \tag{18}$$

where

$$Y_{o1} = \frac{1}{Z_{o1}} = \frac{j\omega C_1}{R_1 + j\omega L_1}$$

$$V_F = \frac{(1-\rho_{11})}{2\Delta_1} V_s\ ,\ V_R = \frac{(1-\rho_{11})}{2\Delta_1} V_s\ \rho_{21}\ e^{-2\gamma_1 \ell}$$

Substituting (11), (12), (17) and (18) into (15) and integrating yields,

$$V_2(0) = -V_R\, A(Y_{o1}Z_{ab} + Y_{ab}Z_{o2})\,(e^{+(\gamma_2+\gamma_1)\ell} - 1)/(\gamma_2+\gamma_1)$$

$$+V_R\, B(Y_{o1}Z_{ab} - Y_{ab}Z_{o2})\,(e^{-(\gamma_2-\gamma_1)\ell} - 1)/(\gamma_2-\gamma_1)$$

$$+V_F\, A(Y_{o1}Z_{ab} - Y_{ab}Z_{o2})\,(e^{+(\gamma_2-\gamma_1)\ell} - 1)/(\gamma_2-\gamma_1)$$

$$-V_F\, B(Y_{o1}Z_{ab} + Y_{ab}Z_{o2})\,(e^{-(\gamma_2+\gamma_1)\ell} - 1)/(\gamma_2+\gamma_1) \qquad (19)$$

and

$$V_2(\ell) = -V_R\, A'(Y_{o1}Z_{ab} + Y_{ab}Z_{o2})\,(e^{+(\gamma_2+\gamma_1)\ell} - 1)/(\gamma_2+\gamma_1)$$

$$+V_R\, B'(Y_{o1}Z_{ab} - Y_{ab}Z_{o2})\,(e^{-(\gamma_2-\gamma_1)\ell} - 1)/(\gamma_2-\gamma_1)$$

$$+V_F\, A'(Y_{o1}Z_{ab} - Y_{ab}Z_{o2})\,(e^{+(\gamma_2-\gamma_1)\ell} - 1)/(\gamma_2-\gamma_1)$$

$$-V_F\, B'(Y_{o1}Z_{ab} + Y_{ab}Z_{o2})\,(e^{-(\gamma_2+\gamma_1)\ell} - 1)/(\gamma_2+\gamma_1) \quad . \qquad (20)$$

Where $Z_{ab} = R_{ab} + j\omega L_{ab}$, $Y_{ab} = j\omega C_{ab}$

$$A = -\rho_{22}\, e^{-2\gamma_2\ell}\, B \quad , \quad B = -\frac{(1+\rho_{12})}{2\Delta_2}$$

$$A' = \frac{(1+\rho_{22})\, e^{-\gamma_2\ell}}{2\Delta_2} \quad , \quad B' = -\rho_{12} * A' \quad .$$

Equations (19) and (20) are resultant forms for the terminal voltage on the receiving line when the driven line is excited at z = 0 by a voltage source.

MEASURED DATA

With Equations (19) and (20) and the possibility of making measurements under various termination conditions, it is evident that sufficient data can be measured to solve for R_{ab}, L_{ab}, and C_{ab} the coupling parameters. To this end, an additional shielding braid was pulled over a

length of RG-214 cable. TDR measurements were made of the velocity of propagation and the cable impedance (Table I). It was noted that the polyvinyl jacket has a velocity of propagation that is somewhat dependent upon frequency; however, an average velocity of 1.63×10^8m/sec was used in all predictions.

Table I

IMPEDANCE CHARACTERISTICS OF RG-214 WITH AN EXTRA SHIELD OVER THE INSULATING JACKET

DC Resistances	Center Conductor	= 7.26 mΩ/m
	Shield	= 8.4 mΩ/m
	Added Shield	= 4.6 mΩ/m
Characteristic Impedances	Interior Circuit	= 50 Ω
	Shield Circuit	= 9.5 Ω
Velocity of Propagation	Interior Circuit	= 1.92×10^8m/sec
	Exterior Circuit	= 1.63×10^8m/sec (at 20 MHz)

In Figure 2 is shown the type of measurement that is often used to measure Z_{ab}. In this case the driver circuit was the interior circuit and the transfer function measured was not Z_{ab} directly, $Z_{ab} = \frac{V_{2o.c.}}{I_{1s.c.}}$, but rather the ratio of two voltages $\left(\frac{V_f}{V_t}\right)$. This ratio is easily related to Z_{ab}, and Y_{ab} by (19) and (20). It was found that if the DC resistance of the shield were used as the value for R_{ab}, a reasonably good fit to the low frequency part of the curve could be made. Further, it was found that one could assume that the high frequency coupling was either inductive or capacitive and obtain equally good comparison to the measured data, provided $L_{ab}Y_{o1} \simeq C_{ab}Z_{o2}$ as suggested by (19) and (20). Further comparisons indicated that these same empirically determined values of L_{ab} and C_{ab} would give equally good fits to the matched driver-matched receiver configuration (Figure 3) and reasonable fits to the data obtained in the Y_{ab} measurement configuration (Figure 4).

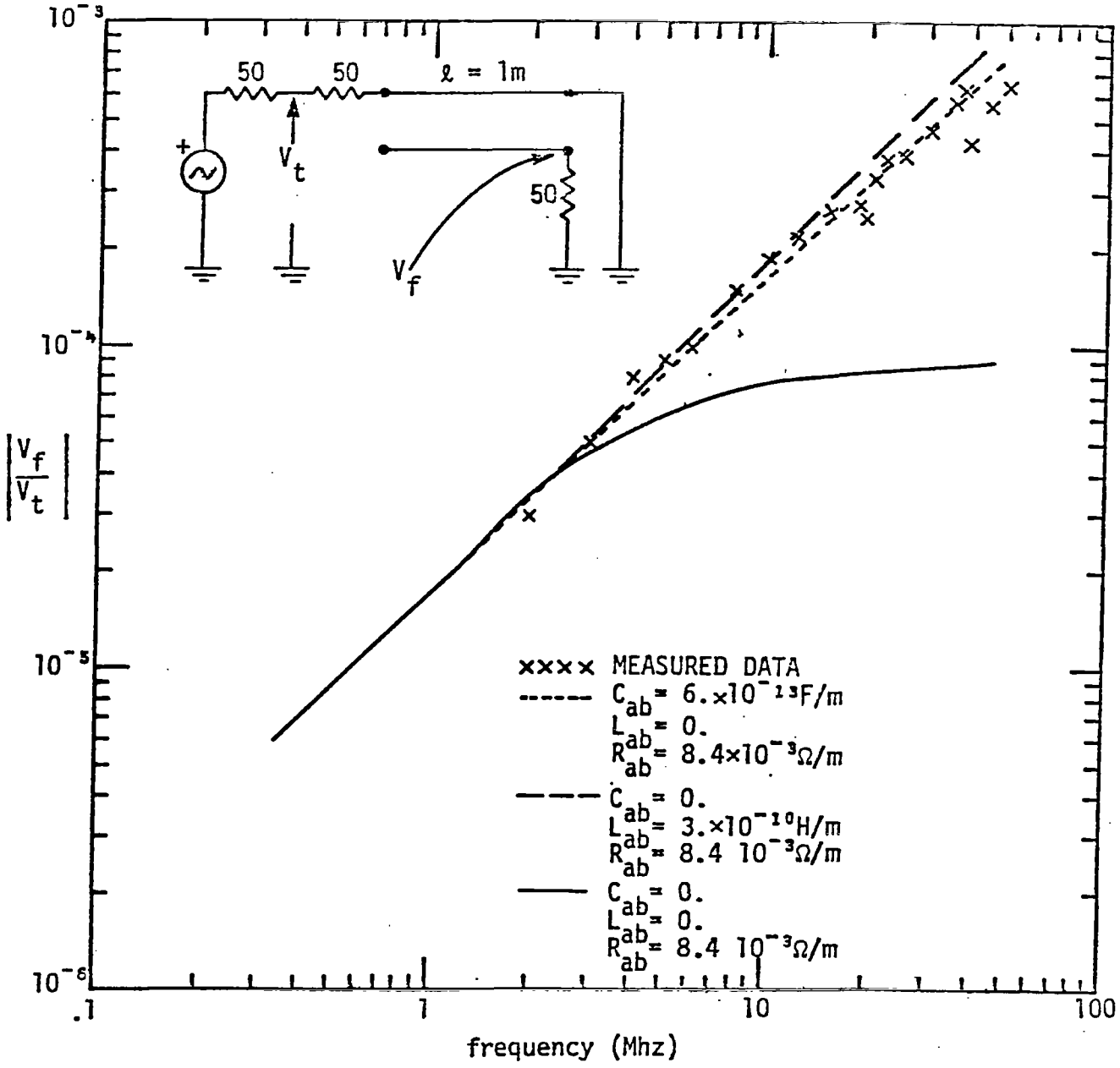

Figure 2. Comparison of measured data and empirical fits for the Z_{ab} measurement configuration of the RG-214 test cable.

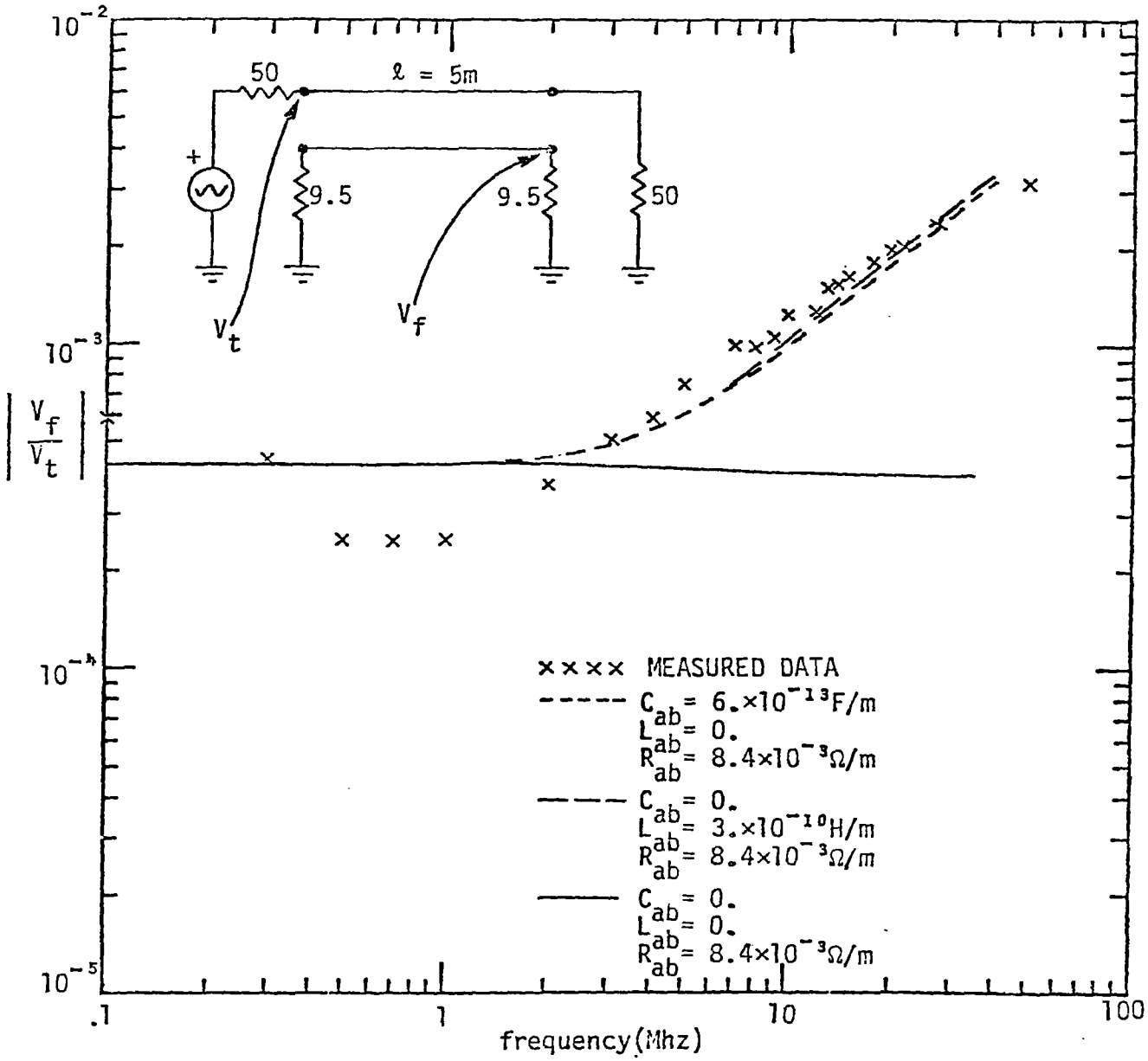

Figure 3. A comparison of measured data and empirical fits for the matched driver-matched receiver configuration of the RG-214 test cable.

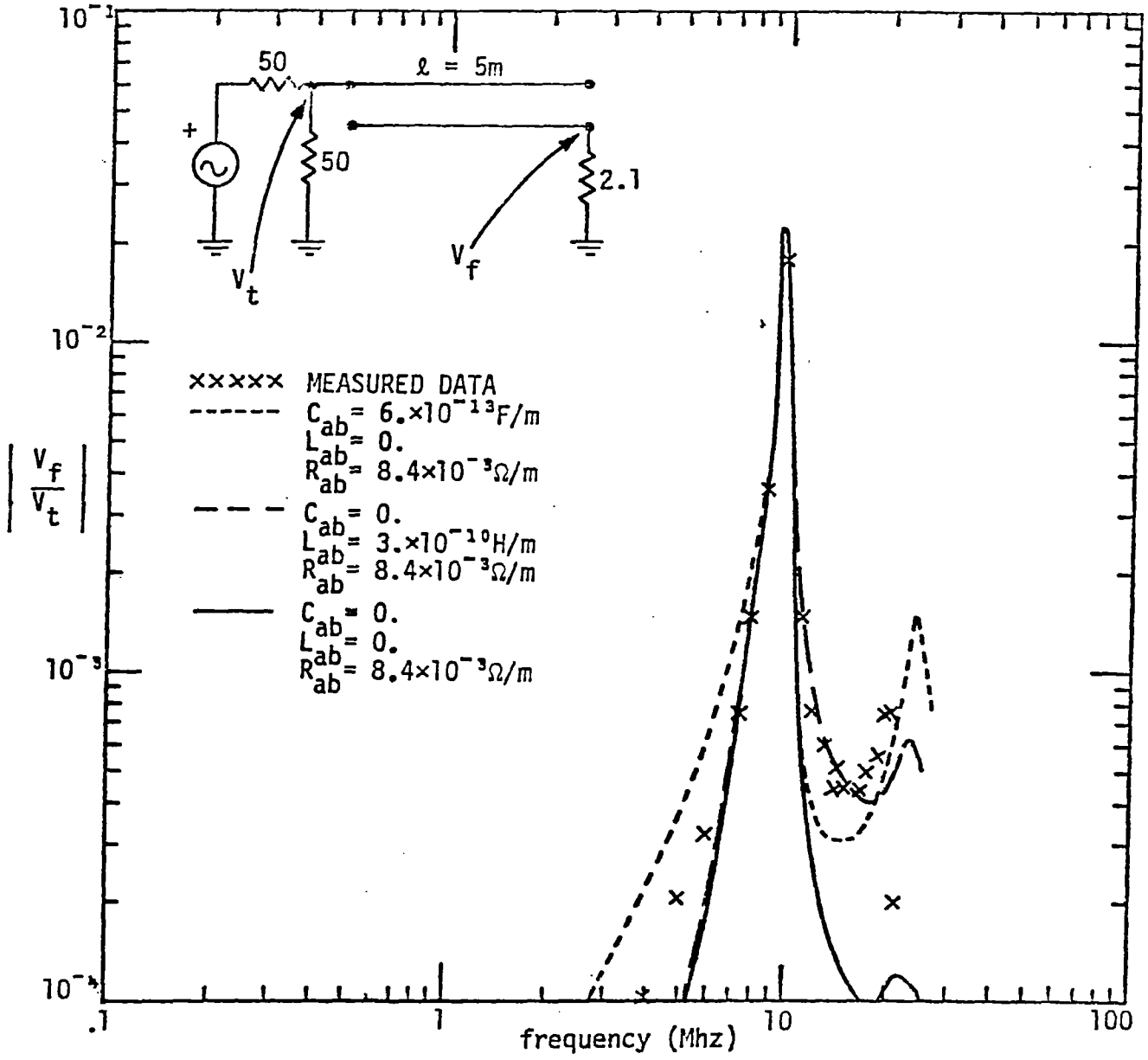

Figure 4. A comparison of measured data and empirical fits for the Y_{ab} measurement configuration of the RG-214 test cable.

Combinations of L_{ab} and C_{ab} were also tried, but the authors found little merit in any combination since the R_{ab}-L_{ab} model or the R_{ab}-C_{ab} model each produced a reasonably accurate fit to all the data.

Pulse measurements were also made using this type of cable and compared to predictions made by Fourier transforming the frequency domain response predicted by (19) and (20) with an appropriate pulse input (Figs. 5-7). Allowing for the fact that the pulse generator had a slower fall time than the numerical driver, and allowing for the frequency dependence of the velocity of propagation of the polyvinyl jacket, we find the agreement between theory and measurement quite acceptable. The very interesting observation is made that the high frequency leakage through the braid only engenders a spike in the waveform and that the polarity of the spike on the far end depends upon the dominant coupling mode through the shield. Perhaps more important is the observation that most of the waveform is due to the mutual resistance term R_{ab} that we have here modeled to acceptable accuracy by the simple DC resistance of the shield.

COMMENT ON THE MEASUREMENT OF SHIELD LEAKAGE

As previously mentioned, the authors found that the measured CW data in Figures 2, 3, and 4 were not adequate to discern the correct magnitude of the mutual inductances and capacitance. The reason for this is that the RG-214 is a reasonably well-shielded cable in the sense that the mutual inductance and mutual capacitance are small. Consequently, high frequencies are needed to make $\omega L_{ab} > R_{ab}$ and $\omega C_{ab} Z_{o2} > R_{ab} Y_{o1}$. At these higher frequencies a 5-meter cable is no longer a small fraction of a wavelength long. With standing waves on the driver cable both mutual inductance and mutual capacitance contribute to the signals observed on the receiving cable in any configuration.

The measurement configuration recommended by the authors is shown in Figure 8. Here the open circuit voltage is to be measured in each case; that is to say, the input impedance of the voltage probe must be much higher than the output impedance of the receiving cable (this could be a problem for the measurement of C_{ab}).

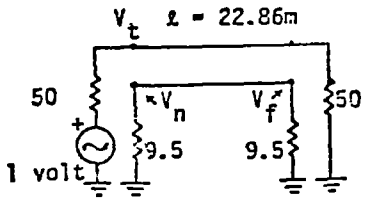

For R-L Coupling Model: R_{ab} = 8.4 mΩ/m, L_{ab} = .3 nanohenries/m, C_{ab} =

For R-C Coupling Model: R_{ab} = 8.4 mΩ/m, L_{ab} = 0., C_{ab} = .6 picofarads/m

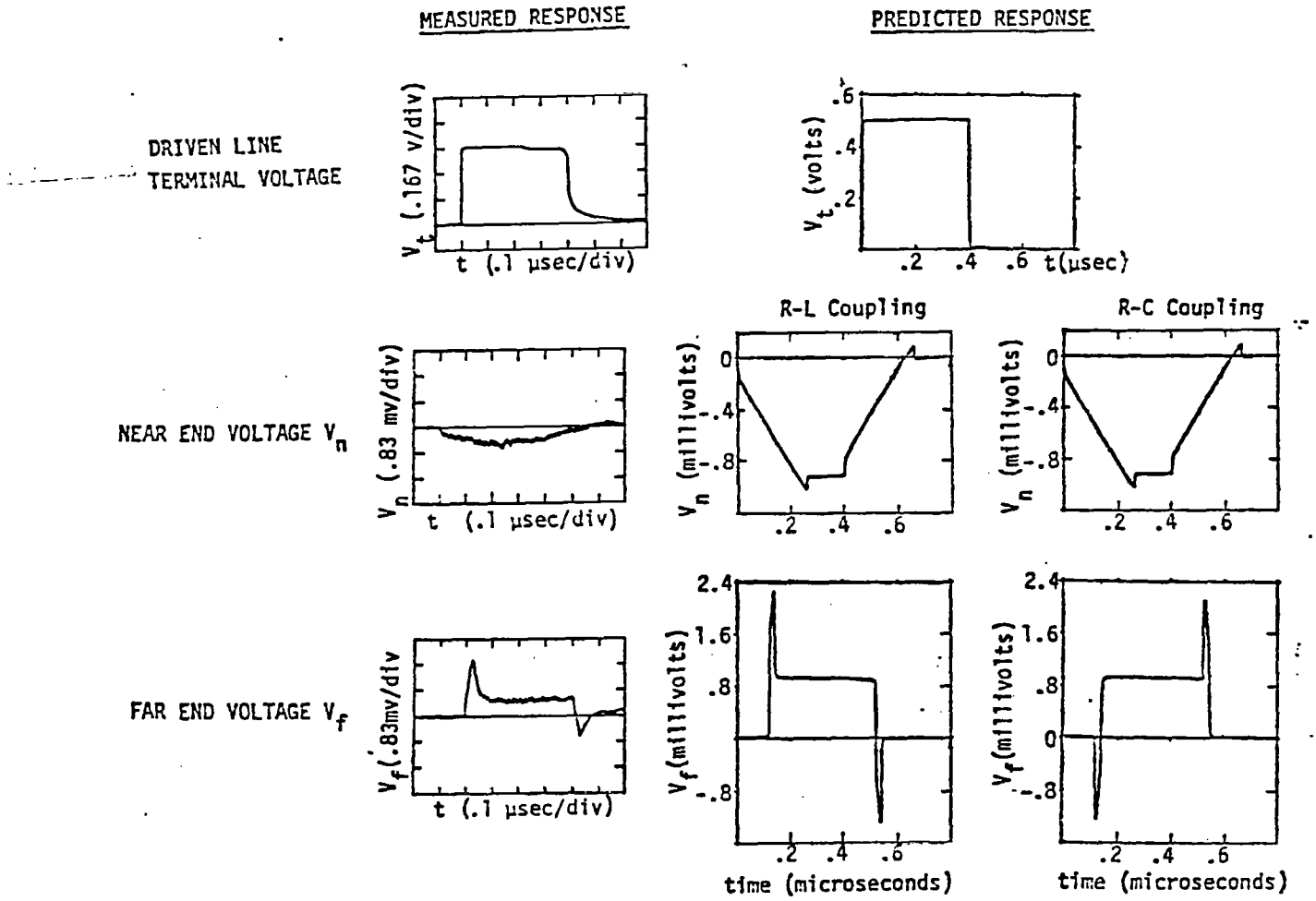

Figure 5. Comparison of measured response with R-L and R-C coupling model predictions for the matched driver and matched receiver configurations of RG-214 test cable.

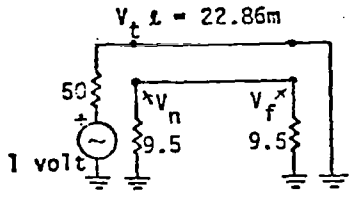

For R-L Coupling Model: R_{ab} = 8.4 mΩ/m, L_{ab} = .3 nanohenries/m, C_{ab} = 0.
For R-C Coupling Model: R_{ab} = 8.4 mΩ/m, L_{ab} = 0., C_{ab} = .6 picofarads/m.

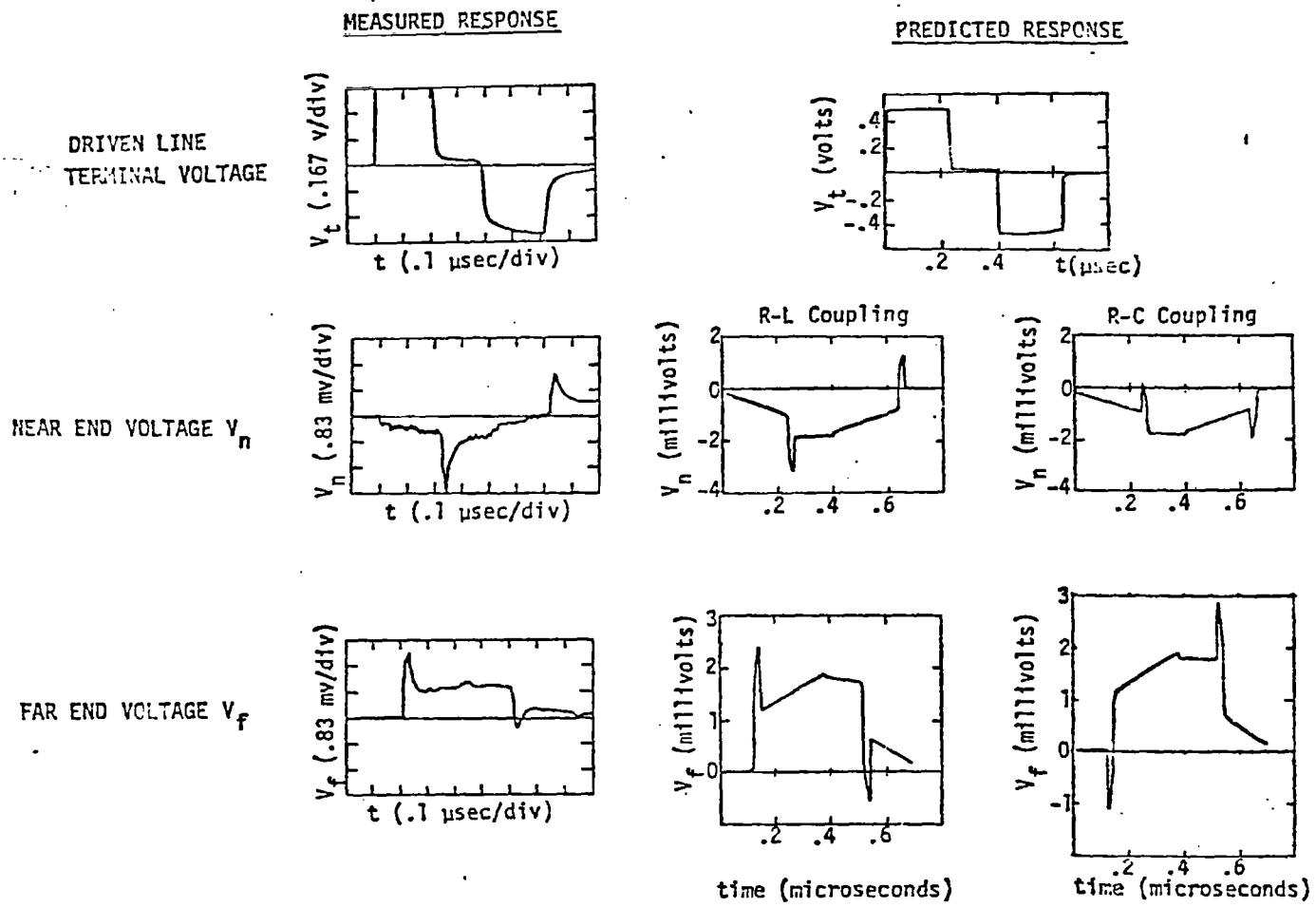

Figure 6. Comparison of measured response with R-L and R-C coupling model predictions for the shorted driver and matched receiver configurations of RG-214 test cable.

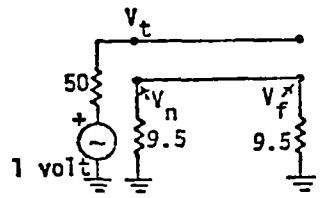

For R-L Coupling Model: R_{ab} = 8.4 mΩ/m, L_{ab} = .3 nanohenries/m, C_{ab} = 0.
For R-C Coupling Model: R_{ab} = 8.4 mΩ/m, L_{ab} = 0., C_{ab} = .6 picofarads/m.

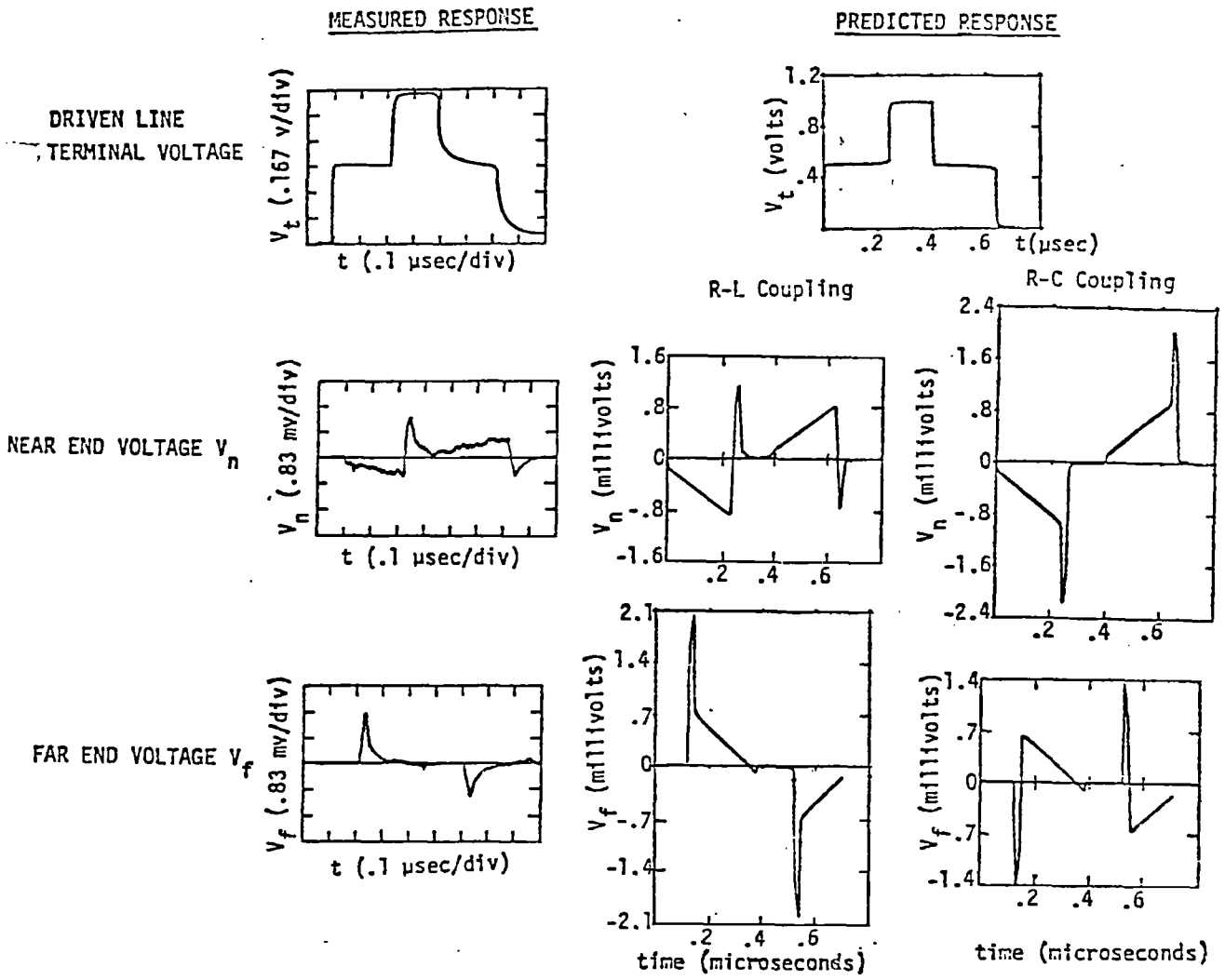

Figure 7. Comparison of measured response with R-L and R C coupling model predictions for the open driver and matched receiver configurations of RG-214 test cables.

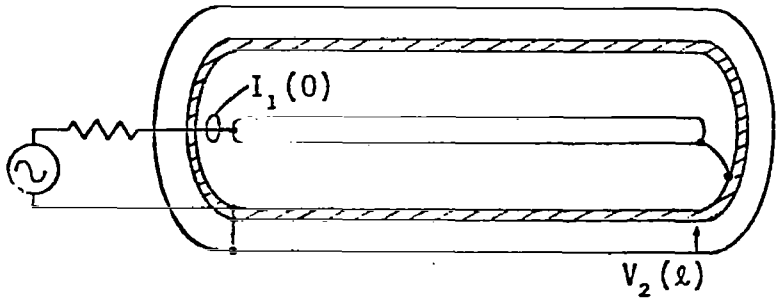

Z_{ab} MEASUREMENT

$$\frac{V_2(\ell)}{I_1(0)} = \left\{ Z_{ab}\ell - Y_{ab}\ell\, Z_{01} Z_{02} \frac{(\gamma_1\ell)(\gamma_2\ell)}{2} \right\}$$

$$\simeq Z_{ab}\ell \text{ if } \gamma_1\ell \ll 1$$

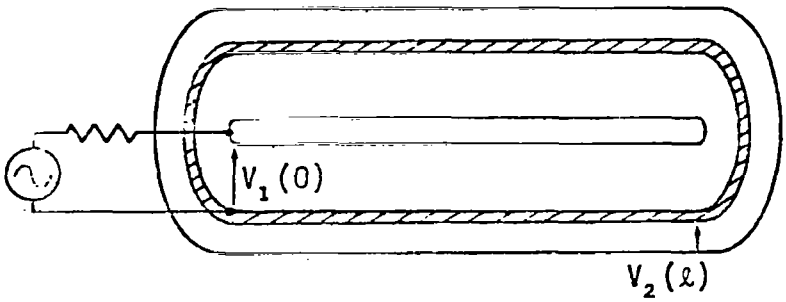

Y_{ab} MEASUREMENT

$$\frac{V_2(\ell)}{V_1(0)} = \left\{ -\frac{C_{ab}}{C_2}\left(1 + \frac{(\gamma_1\ell)^2}{2}\right) + Y_{01}\, Z_{ab}\, \gamma_1\ell \right\}$$

$$= -\frac{C_{ab}}{C_2} \text{ if } \gamma_1\ell \ll 1$$

Figure 8. Measurement configurations for mutual impedance and mutual admittance with second-order formulas for coupling.

Second order formulas for the desired transfer ratios are given showing how cross coupling between terms results.

Ideally, the cable should be cut short enough to make measurements over the entire frequency range of interest. Wide band measurements

also help assure that the mutual capacitance is properly measured. Since the mutual admittance coupling is generally smaller than the mutual impedance coupling, it is difficult to assure that the voltage ratio intended to measure C_{ab}/C_2 is not really $Y_{o1} Z_{ab} \gamma_1 \ell$. This could be particularly troublesome on cables where the mutual resistance is frequency dependent. In that case, the use of the second order equation to determine C_{ab}/C_2 is desirable.

Measurements like those described here were made on the RG-214 test cable. They showed that a more correct mutual resistance would be 5 mΩ/m. These measurements also showed that the mutual capacity was less than .05 picofarads/m.

EXTRAPOLATION OF MEASUREMENTS TO DIFFERENT PROBLEMS

In making the measurements of leakage through the shield braid on the RG-214 cable an additional braid was pulled over the jacket to form an exterior circuit. The question arises then as to how to apply the data taken in this manner to more realistic problems like a cable loosely supported over a ground plane, or a cable laying on the bottom of a horizontal conduit.

Vance [5] has studied the physics of the leakage through holes in the cable shield. He concluded that since the mutual capacitance is determined by a voltage ratio and the coupling is actual electric field coupling, the mutual capacitance is proportional to the incremental capacitance of both the inner and outer circuits

$$C_{ab} = KC_1C_2$$

This relation can be used to transfer data measured in one configuration to a different configuration. The mutual impedance is dependent only upon shield geometry and not upon the line parameters of either the inner or outer circuits.

SUMMARY

In the preceding discussion, we have shown that either mutual inductance or mutual capacitance can couple similar AC signals through shielding

braid on long cables. The transient data augments this conclusion illustrating that high frequency leakage, whether capacitive or inductive, adds spikes to the waveshape; the difference between capacitive and inductive coupling is only the polarity of these superimposed spikes.

An interesting feature of this data is the fact that no skin depth rolloff at low frequencies was used in the predictions of Figures 5-7. Figure 3 indicates that some rolloff might be present with a break frequency of about .3 MHz. However, matching that data with the skin depth rolloff formula used for solid shields [3] or [5] smoothsthe corners of the transient response predictions far more than that exhibited in the measured data. We concluded, therefore, that although there is probably reduction in the coupling due to diffusion at higher frequencies, it does not diminish as rapidly as the diffusion through a solid shield with the same radius and the same DC resistance.

As a conclusion, it is worthwhile to consider an example: suppose a TV antenna is mounted on a chimney and the signal brought into the house on a length of RG-214 cable. Suppose that the antenna is struck by lightning and the stroke travels down the cable for seventy-five feet before being diverted to a ground stake. What is the peak voltage you may expect at the television input terminals?

In this case, transient currents are impressed on the outside of the shield that propagate down the cable away from the stroke. This is the reverse of the case used to obtain the measured data. However, we can obtain the result directly from the measured data by using the reciprocity theorem.

In obtaining the measured data (Figure 1) the internal coaxial cable was driven with a 1-volt square pulse. This drive produced a voltage across Z_{L22} (9.5Ω) of about 8 mv (Figure 5). This means the current flowing through Z_{L22} was $8 \cdot 10^{-3}/9.5 = 8.4 \cdot 10^{-4}$ amps. By reciprocity, a 1-volt generator in series with Z_{L22} would produce .84 ma through Z_{L11}. This completes the application of the theorem. If we then scale the voltage in series with Z_{L22}

up to a voltage which would produce 20,000 amps flowing on the exterior of the shield (an average lightning stroke has a current of 20,000 amps), this would produce a voltage across Z_{L11} of 16 kV since

1 V in series with Z_{L22} → 0.84 mA through Z_{L11}

380 kV in series with Z_{L22} → 20,000 amps on the shield

→ 320 amps through Z_{L11}

(320 amps through Z_{L11} is 16 kV across this 50-Ω resistor).

Note that this voltage is independent of the pulsewidth; the longer the driving pulse, the longer the induced pulse. In fact, this voltage is the minimum that would be observed because it is based on the d.c. resistive coupling and not the reactive coupling. Since the calculation is based upon only the transfer impedance, the extrapolation of the triax data in this case is accurate. Clearly, the front end of the TV set cannot be expected to survive. Since the outside of the sheath was grounded, this is not really a worst case analysis. It does illustrate, however, the importance of grounding the mast of the antenna with a good low inductance ground to divert the stroke from the antenna lead-in.

ACKNOWLEDGMENT

The authors would like to thank D. G. Palmer and Gene Cook, of Sandia Laboratories, for their assistance in this study. D. G. Palmer pointed out the rich character of the transient data and Gene Cook provided all the measured data needed.

REFERENCES

1. Frankel, S., "Terminal Response of Braided-Shield Cables in External Monochromatic Electromagnetic Fields," IEEE Trans. Electromagnetic Compatibility, vol. EMC-16, no. 1, February 1974, pp. 1-16.

2. Merewether, D. E., "A Numerical Solution for the Response of a Strip Transmission Line Over a Ground Plane Excited by Ionizing Radiation," IEEE Trans. Nuc. Sci., vol. NS-18, No. 5, August 1971.

3. Schelkunoff, S. A., "The Electromagnetic Theory of Coaxial Transmission Lines and Cylindrical Shields," Bell System Tech. Jo., vol. 13, October 1934, p. 552.

4. Weeks, Electromagnetic Theory for Engineering Applications, John Wiley & Sons, Inc., New York, 1964, pp. 102-111.

5. Vance, E. F., "Shielding Effectiveness of Braided Wire Shields," IEEE Trans. Electromagnetic Compatibility, vol. EMC-17, no. 2, May 1975, pp. 71-77.